

1

2 Original Article

3

4 Geographic and temporal trends in fentanyl-detected deaths in Connecticut,

5 2009-2019

6

7 Haidong Lu^{1,2}, Forrest W. Crawford^{2,3,4,5,6}, Gregg S. Gonsalves^{1,2,7}, Laretta E. Grau¹

8

9 ¹Department of Epidemiology of Microbial Diseases, Yale School of Public Health, New Haven,

10 CT, USA

11 ²Public Health Modeling Unit, Yale School of Public Health, New Haven, CT, USA

12 ³Department of Biostatistics, Yale School of Public Health, New Haven, CT, USA

13 ⁴Department of Statistics & Data Science, Yale University, New Haven, CT, USA

14 ⁵Department of Ecology & Evolutionary Biology, Yale University, New Haven, CT, USA

15 ⁶Yale School of Management, New Haven, CT, USA

16 ⁷Yale Law School, New Haven, CT, USA

17 **Running title:** Trends in fentanyl-detected deaths in Connecticut

18 **Correspondence:** Gregg Gonsalves

19 Public Health Modeling Unit and Department of Epidemiology of Microbial

20 Diseases

21 Yale School of Public Health

22 350 George Street, Ste 3rd Floor

23 New Haven, CT 06511

24 Phone: +1 (203) 606-9149

25 gregg.gonsalves@yale.edu

26 **Funding sources:** National Institutes of Health/National Institute on Drug Abuse DP2-DA049282

27 and R37DA15612); National Institutes of Health/Eunice Kennedy Shriver

28 National Institute of Child Health and Human Development DP2-HD091799

29 **Conflict of interest:** None declared.

30 **Data and code:** Data are available on request to the authors.

31 **Word count:** abstract 197/200; main text 3091/3000

32 **Acknowledgements:** We are grateful to Dr. James R. Gill and his staff at the Connecticut Office

33 of the Chief Medical Examiner for providing access to data. In addition, we

34 thank Joshua L. Warren, Thomas A. Thornhill, Julia Dennett, and A Ram for

35 helpful comments.

36

37 **ABSTRACT**

38 **Purpose:** Since 2012 fentanyl-detected fatal overdoses have risen from 4% of all fatal overdoses
39 in Connecticut to 82% in 2019. We aimed to investigate the geographic and temporal trends in
40 fentanyl-detected deaths in Connecticut during 2009-2019.

41 **Methods:** Data on the dates and locations of accidental/undetermined opioid-detected
42 fatalities were obtained from Connecticut Office of the Chief Medical Examiner. Using a
43 Bayesian space-time binomial model, we estimated spatiotemporal trends in the proportion of
44 fentanyl-detected deaths.

45 **Results:** During 2009-2019, a total of 6,632 opioid deaths were identified. Among these, 3,234
46 (49%) were fentanyl-detected. The modeled spatial patterns suggested that opioid deaths in
47 northeastern Connecticut had higher probability of being fentanyl-detected, while New Haven
48 and its neighboring towns and the southwestern region of Connecticut, primarily Greenwich,
49 had a lower risk. Model estimates also suggested fentanyl-detected deaths gradually overtook
50 the preceding non-fentanyl opioid-detected deaths across Connecticut. The estimated temporal
51 trend showed the probability of fentanyl involvement increased substantially since 2014.

52 **Conclusion:** Our findings suggest that geographic variation exists in the probability of fentanyl-
53 detected deaths, and areas at heightened risk are identified. Further studies are warranted to
54 explore potential factors contributing to the geographic heterogeneity and continuing
55 dispersion of fentanyl-detected deaths in Connecticut.

56 **Keywords:** fentanyl; overdose; opioid crisis; Bayesian disease mapping; spatiotemporal analysis

57

58

59 INTRODUCTION

60 The three waves of the American opioid crisis (i.e., prescription opioids, heroin, and synthetic
61 opioids other than methadone) continue to be a significant public health emergency in the
62 United States (US).¹ Beginning in late 2013, synthetic opioid overdoses (chiefly illicitly produced
63 fentanyl and fentanyl analogs) have dominated the ongoing third wave of the opioid crisis.²
64 Illicit drug supply is the key driver of the current opioid crisis.³ Illicitly manufactured fentanyl
65 and fentanyl analogs, which are less costly to produce and distribute (but are 50 to 100 times
66 more potent than morphine),⁴ have increased in the US drug market.⁵ Reports from the US
67 Drug Enforcement Administration highlighted the dramatic increase in drug seizures that tested
68 positive for fentanyl, from 4,642 in 2014 to 98,954 in 2019 in the US.^{6,7} The national rate of
69 drug overdose deaths involving fentanyl increased dramatically from 0.5 per 100,000 persons in
70 2011 to 5.9 per 100,000 in 2016.⁸ From 2014 to 2015, overdose deaths attributed to synthetic
71 opioids (primarily illicitly manufactured fentanyl) increased by 72% to nearly 10,000.⁹ Most
72 recently, the rate of drug overdose deaths involving synthetic opioids rose by 27%, from 9.0 per
73 100,000 in 2017 to 11.4 in 2019.^{10,11} In 2018, fentanyl and its analogs were detected in
74 approximately two thirds of opioid deaths.¹²

75
76 Abrupt-changes in illicit drug supply may have contributed to the heightened risk of opioid
77 overdoses since 2013 and the influx of fentanyl.³ Examining the spatiotemporal trends of
78 fentanyl-detected deaths may help public health researchers and policymakers better
79 understand geographic and temporal variation in fentanyl availability. While several studies
80 have been conducted to investigate the small-area geographic distribution of fentanyl-detected

81 overdose deaths^{13,14}, to our knowledge, no research has explored whether the fentanyl-
82 detected overdose deaths simply take over the rising overall opioid overdoses in the same
83 geographic region or whether fentanyl has established new regions of risk for overdose where,
84 previously, overdoses were less common.

85
86 To further inform overdose prevention and intervention efforts, we investigated the geographic
87 and temporal trends of fentanyl-detected overdose deaths at the city/town level in Connecticut,
88 a state that is highly affected by the opioid crisis. We examined whether spatiotemporal
89 distributions of fentanyl-detected overdose deaths covary with overall trends of opioid
90 overdose deaths, and whether the rising tide of fentanyl-detected overdose deaths follows a
91 geographic pattern different from that of the preceding wave of opioid overdose deaths. Our
92 town-level estimates will help support the decision-making of the local health agencies
93 (organized by town or health districts consisting of several towns) in Connecticut on public
94 health and surveillance efforts to address the opioid crisis.

95

96 **METHODS**

97 *Study Sample and Data*

98 We obtained data on all opioid-detected overdose deaths from the records of the Connecticut
99 Office of the Chief Medical Examiner (OCME), including the cause and manner of death,
100 toxicological test results in available specimens, demographic information (i.e., age, sex,
101 race/ethnicity), and the addresses of residence, injury, and/or death for each case.^{15,16} In the
102 OCME records, “opioid detection” in an overdose death means that either an opioid was listed

103 in the cause of death or that a quantifiable amount of an opioid was present in the toxicological
104 test report.

105
106 All opioid-detected overdose deaths from 2009 to 2019 in Connecticut that the OCME
107 determined to be of accidental or undetermined manner were included in this analysis. Non-
108 residents in Connecticut were excluded. We dichotomized the opioids detected in the overdose
109 deaths (i.e., fentanyl-detected versus non-fentanyl-detected). Other substances of interest
110 included heroin/morphine, pharmaceutical opioids (i.e., di-hydrocodeine, hydromorphone,
111 hydrocodone, hydromorphone, oxymorphone, and tramadol), methadone/buprenorphine,
112 benzodiazepines, cocaine, ethanol, methamphetamine, xylazine, mitragynine (kratom), and
113 gabapentin. This research project has been reviewed by the Connecticut OCME and deemed
114 not human subjects research by the Yale University Human Investigations Committee.

115
116 *Geospatial Data*

117 All residential, injury, and death addresses were geocoded within ArcGIS (ESRI, Redlands, CA).
118 Unmatched addresses were then reviewed manually and geocoded using ArcGIS or the R
119 package *tidygeocoder*¹⁷. In cases where decedents were listed as homeless or where no address
120 was recorded, these cases were not geocoded. Decedents with residential addresses outside
121 Connecticut were excluded. Injury addresses were used as primary locales for the space-time
122 model and mapping the spatial trends. If injury addresses were unknown, residential addresses
123 were used instead. If both addresses were unknown, death addresses were used. The geocoded

124 overdose deaths were then assigned to one of the 169 corresponding cities or towns in
125 Connecticut.

126

127 *Covariates*

128 We used demographic information available for residential population at the city/town level in
129 the Connecticut from the American Community Survey (ACS).¹⁸ We linked these with the
130 city/town-level ACS 5-year estimates from 2015-2019 data and 2010-2014 data to the opioid-
131 detected overdose death records in 2015-2019 and in 2009-2014, respectively. The covariates
132 were the total population size, proportion of the population by demographic covariates (i.e.,
133 age groups, sex, race, ethnicity and education level), proportion foreign born, the proportion
134 with home ownership, median household income, and poverty rate.

135

136 *Statistical Analyses*

137 We first described demographic information of the decedents with opioid-detected fatal
138 overdoses in Connecticut, stratified by fentanyl-detected overdose deaths and non-fentanyl
139 overdose deaths. Then we examined spatiotemporal trends in counts of opioid-detected
140 overdose deaths within towns in Connecticut. We modelled the count of opioid-detected
141 overdose deaths n_{it} in town i during year t as independently and identically Poisson distributed
142 variables with mean λ_{it} ,

$$n_{it} \sim \text{Poisson}(\lambda_{it})$$

143 The logarithm of the mean number of opioid-detected overdose deaths (λ_{it}) was then modeled
144 as

$$\log(\lambda_{it}) = \mathbf{x}_{it}^T \boldsymbol{\beta} + \alpha_i + \gamma_t + \delta_{it} + \log(\text{pop}_n)$$

145 where \mathbf{x}_{it} is the vector of covariates for town i at year t (including the time-varying and space-
146 varying variables from the ACS), and $\boldsymbol{\beta}$ is a vector of fixed effect coefficients for \mathbf{x}_{it} . In addition,
147 α_i is the town-level spatial main effect, γ_t is the yearly temporal main effect, and δ_{it} is the
148 interaction term between space (town level) and time (year). The population size in each
149 city/town was included as an offset $\log(\text{pop}_n)$ for the Poisson model. The spatial term α_i is a
150 random effect that follows the conditional autoregressive model proposed by Besag, York and
151 Mollie.¹⁹ The random effect can be further decomposed into two components, an intrinsic
152 conditional autoregressive term that smooths each city/town-level estimate by forming a
153 weighted average with all adjacent jurisdictions, plus a spatially unstructured component that
154 models independent location-specific error and is assumed to be independently, identically,
155 and normally distributed across cities or towns. The temporal trend γ_t is modeled by the sum of
156 two components, a first-order random walk-correlated time component, and a temporally
157 unstructured component that models independent year-specific error and is independently,
158 identically, and normally distributed across calendar years. The space-time interaction term δ_{it} ,
159 is modelled as an independent noise term for each city/town and time period and allows for
160 temporal trends in a given city/town to deviate from the overall spatial and temporal trends
161 given by α_i and γ_t , so that local patterns can emerge across time and space. Gamma priors
162 were assigned to the precision hyperparameters in our models. Details of the model
163 specification are described in Appendix S1. It should be noted that here we aimed to model the
164 mean count of opioid-detected overdose deaths in each town during each year, and therefore
165 we directly included λ_{it} in the Poisson model rather than decompose λ_{it} into expected number

166 and relative risk. In addition, given that there were a considerable number of towns with no
167 opioid overdose deaths especially in the earlier years during the study period, we implemented
168 the zero-inflated Poisson model to account for excess zeroes. The model comparison of the
169 Poisson and zero-inflated Poisson models are shown in Appendix S2. We also conducted a
170 sensitivity analysis that used penalized complexity (PC) priors^{20,21} to the precision
171 hyperparameters instead of gamma priors (see Appendix S3).

172
173 To investigate the conditional probability of fentanyl detection given that a fatal opioid-
174 involved overdose occurred, we modelled the probability of an opioid overdose death being
175 fentanyl-detected at the city/town level, using a Bayesian space-time binomial model.²² Unlike
176 the Poisson regression directly modeling the count data, the binomial model represents the
177 probability of fentanyl detection given an opioid-detected death. This can tell us whether the
178 conditional risk of fentanyl detection, given an opioid fatal overdose, varies over space and time.
179 Specifically, we considered a binomial model for the number of fentanyl-detected overdose
180 deaths conditional on the total number of opioid overdose deaths in the town areas. Let p_{it} be
181 the probability of an opioid overdose death being fentanyl-detected in town i during year t . We
182 assumed that the number of fentanyl-detected overdose deaths y_{it} in town i during year t is
183 distributed as

$$y_{it} \sim \text{Binomial}(p_{it}, n_{it})$$

184 and the corresponding likelihood is

$$185 \quad L(y_{it}|p_{it}, n_{it}) = \prod_i \prod_t \binom{n_{it}}{y_{it}} p_{it}^{y_{it}} (1 - p_{it})^{(n_{it}-y_{it})}.$$

186 A logistic regression was used to model the probability p_{it} , as

$$\text{logit}(p_{it}) = \mathbf{x}_{it}\boldsymbol{\theta} + \mu_i + \varphi_t + \sigma_{it}$$

187 where, similar to model for opioid-detected overdose deaths, \mathbf{x}_{it} is the vector of covariates for
188 city/town i at year t (including the time-varying and space-varying variables from the ACS), and
189 $\boldsymbol{\theta}$ is a vector of fixed effect coefficients for \mathbf{x}_{it} . In addition, μ_i in the model is the city/town-level
190 spatial main effect, φ_t is the yearly temporal main effect, and σ_{it} is the interaction term
191 between space (city/town level) and time (year). In addition, we conducted three sensitivity
192 analyses to assess the robustness of our results: 1) as an alternative, we constructed a Poisson
193 model for counts of fentanyl-detected overdose deaths among opioid overdose deaths; 2) we
194 restricted the analytical sample to adult (aged ≥ 18) opioid-detected overdose deaths; 3) we
195 used PC priors to the precision hyperparameters instead of gamma priors.

196
197 Finally, we used likelihood ratio tests to examine whether the space-time interaction terms
198 were significantly different from zero in all models. When this term is not significantly different
199 from zero, it suggests that the geographic pattern of fentanyl-detected overdose deaths does
200 not vary significantly over the study period.

201
202 To estimate Bayesian model parameters, we employed integrated nested Laplace
203 approximations (INLAs) which approximate the full posterior distribution and are a
204 computationally efficient alternative to Markov Chain Monte Carlo.²³ Briefly, under certain
205 models (e.g., latent Gaussian models), INLA approximates the marginal posterior distribution of
206 estimated parameters using a multivariate normal distribution.^{23,24} We used the *R-INLA*
207 package for model fitting and estimation.²⁵ Model comparison was performed, and details can

208 be found in Appendix S2. All analyses were performed using R Statistical Software (version 4.0.2;
209 R Foundation for Statistical Computing, Vienna, Austria).

210

211 **RESULTS**

212 A total of 6,632 opioid-detected overdose deaths were identified by the Connecticut OCME
213 between 2009 and 2019, after excluding 27 deaths with residential addresses outside
214 Connecticut. Among these, 3,234 (49%) were fentanyl-detected, and 3,398 (51%) were non-
215 fentanyl-detected fatalities. The characteristics of these overdose deaths are described in Table
216 1. People who died of fentanyl-detected overdose deaths were more likely to be male, Black,
217 Hispanic, or involve at least one of the following substances: cocaine, xylazine, gabapentin or
218 mitragynine, compared with those who died of non-fentanyl-detected overdose. The
219 characteristics of overall opioid-detected overdose deaths as well as fentanyl-detected
220 overdose deaths stratified by calendar year are shown in Appendix S4.

221

222 Figure 1 shows the observed temporal trend of fentanyl-detected overdose deaths and non-
223 fentanyl overdose deaths in Connecticut during the study period 2009-2019. Fentanyl-detected
224 overdose deaths increased significantly since 2014. In 2019, 977 (86%) of the 1,138 opioid-
225 detected overdose deaths were fentanyl-detected, compared to 15 (6%) of 266 opioid-detected
226 overdose deaths in 2009 and 36 (8%) of 429 opioid-detected overdose deaths in 2013. The
227 yearly geographic patterns of observed proportion being fentanyl-detected among opioid-
228 detected overdose deaths at the town level are shown in Appendix S5.

229

230 Model comparison of the Poisson and zero-inflated Poisson models supported the choice of
231 Poisson model (see Appendix S2). Posterior distributions of estimated parameters for spatial
232 (α_i) and temporal (γ_t) random effects (while holding other terms constant) of Bayesian space-
233 time Poisson model for overall opioid-detected overdose deaths are shown in Figure 2. Some
234 towns – Torrington and Southington – were at heightened risk of opioid-detected overdose
235 deaths. The temporal trends showed the risk of opioid-detected overdose deaths among
236 residents in Connecticut increased substantially from 2009 to 2019, although there was a slight
237 decrease in 2018.

238
239 Based on the fitted Bayesian space-time binomial model for the proportion of fentanyl-
240 detected overdose deaths, posterior distributions of the fixed-effect coefficients (θ) of
241 covariates are summarized in Figure 3. Increased proportion of residents aged 55-64 in a
242 city/town was associated with decreased probability being fentanyl-detected, given an opioid-
243 detected overdose death in that town, with an odds ratio (OR) of 0.92 (95% credible interval
244 [CrI], 0.86, 0.99). In addition, the proportion in poverty was negatively associated with the
245 probability of a fatal overdose being fentanyl-detected (OR=0.95 [95% CrI, 0.91, 0.99]).

246
247 Posterior distributions of estimated parameters for spatial (μ_i) and temporal (φ_t) random
248 effects (while holding other terms constant) are summarized in Figure 4, along with geographic
249 patterns across towns. Some areas had increased probability of fentanyl involvement, and the
250 spatial modeling (holding temporal terms constant) suggests that even after adjusting for the
251 city/town level demographic covariates, the northeastern region of Connecticut had a higher

252 probability of fentanyl-detected deaths, with Hartford, East Hartford and Manchester at the
253 highest risk. In contrast, New Haven and its surrounding towns and the southwestern
254 Connecticut—primarily Greenwich—had a lower probability of fentanyl-detected deaths. The
255 temporal trends in Figure 4 describe main temporal trends similar to those observed in Figure 1,
256 that is, that the probability of an opioid overdose death being fentanyl-detected increased
257 monotonically since 2014.

258
259 The city/town-level predicted probabilities of being a fentanyl-detected overdose death from
260 the Bayesian space-time binomial model are shown in Figure 5. A higher probability being
261 fentanyl-detected, given an opioid overdose death, was first found in several towns in the
262 northeastern region of Connecticut during 2009-2013. Beginning in 2014, the fentanyl
263 “hotspots” started to spread across Connecticut.

264
265 A likelihood ratio test shows that the space-time interaction term of the Bayesian space-time
266 binomial model for the proportion of fentanyl-detected opioid overdose deaths was not
267 significantly different from zero, suggesting the geographic patterns of fentanyl-detected
268 overdose deaths gradually overtook the preceding non-fentanyl opioid overdose deaths.

269
270 The results of the sensitivity analyses 1) using Poisson model for fentanyl-detected overdose
271 deaths in Connecticut, 2) restricting to adult opioid-detected overdose deaths, or 3) using PC
272 priors for prior distribution of hyperparameters were similar to those using a binomial logistic
273 model and are described in Appendix S6.

274

275 **DISCUSSION**

276 In the present study we examined the town-level geographic patterns and yearly temporal
277 trends of fentanyl-detected overdose deaths among Connecticut residents during 2009-2019
278 and evaluated the relationship of fentanyl-detected overdose deaths with overall trends of
279 opioid-detected overdose deaths. To our knowledge, this is the first study to map the
280 spatiotemporal distributions of fentanyl-detected overdose deaths in Connecticut. We
281 identified regions of Connecticut, particularly in the northeastern part of the state, as having
282 relatively high probability of an opioid overdose death being fentanyl-detected. The temporal
283 trends show the fentanyl-detected overdose deaths in Connecticut increased significantly since
284 2014. We also found that the geographic pattern of fentanyl-detected overdose deaths was
285 relatively constant over time and gradually replaced the preceding wave of opioid overdose
286 deaths.

287

288 Our findings show that, compared with non-fentanyl overdose deaths, people who died of
289 fentanyl-detected overdose are more likely to be Black or Hispanic in Connecticut, suggesting
290 that these groups are disproportionately affected by the most recent waves of opioid crisis.
291 These results are consistent with the findings from previous studies that examined opioid-
292 detected overdose deaths in other regions and across the US.²⁶⁻²⁸ More research is warranted
293 to address the social determinants of fentanyl-detected overdose deaths among Black and
294 Hispanic communities, and locally informed harm reduction efforts and services should be
295 targeted to these populations.

296

297 Our results indicated that the northeastern region of Connecticut had higher probability of an
298 opioid overdose death being fentanyl-detected whereas New Haven, its surrounding towns,
299 and the southwestern Connecticut had a lower probability. This suggests that the Connecticut
300 supply of fentanyl and its analogues may have originally entered Connecticut from the north,
301 gradually diffused from the northeastern to southwestern Connecticut, and most recently has
302 dispersed across the state. Our findings also suggest that the fentanyl-detected overdose
303 deaths might have simply replaced the preceding waves of opioid overdose deaths (e.g., heroin),
304 rather than creating new overdose risk following distinct geographic patterns. These findings
305 were in line with the facts that fentanyl and its analogues entered into illicit drug supply as an
306 “adulterant” in powder heroin and counterfeit pills in Northeast.²⁹ The growing presence and
307 strong potency of fentanyl and its analogues then led to the significant increase in opioid
308 overdose deaths across Connecticut in recent years.

309

310 Further studies are warranted to explore the potential factors (e.g., supply-side aspects,
311 neighborhood characteristics, and availability and accessibility of health services and naloxone
312 distribution) that result in geographical variability in fentanyl-detected overdose mortality. For
313 example, a recent study in Canada showed the rural areas experienced a disproportionately
314 high risk of fatal overdoses from illicit drug poisoning compared with urban areas.³⁰ Such rural-
315 urban differences may be due to limited access to harm reduction services and rising local drug
316 toxicity. Our study provides insight into the distinctive geographic patterns in fentanyl mortality
317 in Connecticut. These findings can inform targeted overdose surveillance in specific regions of

318 the state and guide more efficient deployment of harm reduction services and opioid treatment
319 programs in Connecticut.

320

321 Our study is subject to several limitations. First, although we adjusted for city/town-level
322 demographic covariates in our Bayesian space-time models, it is possible that this ecological
323 analysis obscures individual-level relationships between time, place, and overdose risk. We
324 described the geographic patterns and temporal trends of fentanyl-detected overdose deaths
325 at the city/town level only and could not examine in detail the potential social determinants for
326 an opioid overdose death being fentanyl-detected. Second, we primarily used injury addresses
327 for the geographic locales and used residential or death addresses only when injury address
328 was missing, which may lead to geographical misclassification. However, most deaths occurred
329 within person's own residence so that the injury and residential addresses were the same.
330 Moreover, death addresses were often in the hospital near the injury place. Therefore, we
331 expect that the influence of geographic misclassification on our study findings was minimal.
332 Lastly, while we investigated the spatiotemporal trends of fentanyl-detected overdose deaths,
333 we did not explore the trends of overdose deaths that involved both fentanyl and other
334 substances such as methamphetamine. Further studies are needed to investigate the
335 spatiotemporal trends of polysubstance use with fentanyl in Connecticut.

336

337 In conclusion, given the high probability of an overdose death being fentanyl-detected, more
338 research should be devoted to exploring the social determinants and supply-side drivers of

339 fentanyl-involved overdose deaths in order to better inform future harm reduction services and
340 policies to halt the current opioid crisis.

341

342

343 **REFERENCES:**

- 344 1. Ciccarone D. The triple wave epidemic: Supply and demand drivers of the US opioid
345 overdose crisis. *Int J Drug Policy*. 2019;71:183-188. doi:10.1016/j.drugpo.2019.01.010
- 346 2. Dasgupta N, Beletsky L, Ciccarone D. Opioid Crisis: No Easy Fix to Its Social and Economic
347 Determinants. *Am J Public Health*. 2018;108(2):182-186. doi:10.2105/AJPH.2017.304187
- 348 3. Zoorob M. Fentanyl shock: The changing geography of overdose in the United States. *Int*
349 *J Drug Policy*. 2019;70:40-46. doi:10.1016/j.drugpo.2019.04.010
- 350 4. Suzuki J, El-Haddad S. A review: Fentanyl and non-pharmaceutical fentanyls. *Drug Alcohol*
351 *Depend*. 2017;171:107-116. doi:10.1016/j.drugalcdep.2016.11.033
- 352 5. Prekupec MP, Mansky PA, Baumann MH. Misuse of Novel Synthetic Opioids: A Deadly
353 New Trend. *J Addict Med*. 2017;11(4):256-265. doi:10.1097/ADM.0000000000000324
- 354 6. Division USDEADC. National Forensic Laboratory Information System: 2014 Annual
355 Report. Published online 2014.
- 356 7. U.S. Drug Enforcement Administration Diversion Control Division. National Forensic
357 Laboratory Information System:NFLIS-Drug 2019 Annual Report. Published online 2019.
358 [https://www.nflis.deadiversion.usdoj.gov/DesktopModules/ReportDownloads/Reports/](https://www.nflis.deadiversion.usdoj.gov/DesktopModules/ReportDownloads/Reports/NFLIS-Drug-AR2019.pdf)
359 [NFLIS-Drug-AR2019.pdf](https://www.nflis.deadiversion.usdoj.gov/DesktopModules/ReportDownloads/Reports/NFLIS-Drug-AR2019.pdf)
- 360 8. Spencer MR, Warner M, Bastian BA, et al. Drug Overdose Deaths Involving Fentanyl,
361 2011-2016. *Natl Vital Stat Reports*. 2018;68(3).
362 [https://stacks.cdc.gov/view/cdc/77832%0Ahttps://www.cdc.gov/nchs/products/index.ht](https://stacks.cdc.gov/view/cdc/77832%0Ahttps://www.cdc.gov/nchs/products/index.htm)
363 [m.](https://stacks.cdc.gov/view/cdc/77832%0Ahttps://www.cdc.gov/nchs/products/index.htm)
- 364 9. Rudd RA, Seth P, David F, Scholl L. Increases in Drug and Opioid-Involved Overdose

- 365 Deaths — United States. *Morb Mortal Wkly Rep.* 2016;65:1445-1452.
- 366 10. Hedegaard H, Miniño AM, Warner M. Drug Overdose Deaths in the United States, 1999-
367 2018. *NCHS Data Brief.* 2020;356.
- 368 11. Mattson CL, Tanz LJ, Quinn K, Kariisa M, Patel P, Davis NL. Morbidity and Mortality
369 Weekly Report Trends and Geographic Patterns in Drug and Synthetic Opioid Overdose
370 Deaths-United States, 2013-2019. *Morb Mortal Wkly Rep.* 2021;70(6):202-207.
371 <https://www.cdc.gov/nchs/data/nvsr/nvsr61/>
- 372 12. Gladden RM, O'Donnell J, Mattson CL, Seth P. Changes in Opioid-Involved Overdose
373 Deaths by Opioid Type and Presence of Benzodiazepines, Cocaine, and
374 Methamphetamine — 25 States, July–December 2017 to January–June 2018. *MMWR*
375 *Morb Mortal Wkly Rep.* 2019;68(34):737-744. doi:10.15585/mmwr.mm6834a2
- 376 13. Marshall BDL, Krieger MS, Yedinak JL, et al. Epidemiology of fentanyl-involved drug
377 overdose deaths: A geospatial retrospective study in Rhode Island, USA. *Int J Drug Policy.*
378 2017;46:130-135. doi:10.1016/j.drugpo.2017.05.029
- 379 14. Nesoff ED, Branas CC, Martins SS. The geographic distribution of fentanyl-involved
380 overdose deaths in Cook County, Illinois. *Am J Public Health.* 2020;110(1):98-105.
381 doi:10.2105/AJPH.2019.305368
- 382 15. Rhee TG, Ross JS, Rosenheck RA, Grau LE, Fiellin DA, Becker WC. Accidental drug
383 overdose deaths in Connecticut, 2012–2018: The rise of polysubstance detection? *Drug*
384 *Alcohol Depend.* 2019;205(September):107671. doi:10.1016/j.drugalcdep.2019.107671
- 385 16. Green TC, Grau LE, Carver HW, Kinzly M, Heimer R. Epidemiologic trends and geographic
386 patterns of fatal opioid intoxications in Connecticut, USA: 1997-2007. *Drug Alcohol*

- 387 *Depend.* 2011;115(3):221-228. doi:10.1016/j.drugalcdep.2010.11.007
- 388 17. Cambon J. Package 'tidygeocoder.' CRAN. Published online 2021:2-13.
- 389 18. Bureau UC. American Community Survey Data. [https://www.census.gov/programs-](https://www.census.gov/programs-surveys/acs/data.html)
- 390 [surveys/acs/data.html](https://www.census.gov/programs-surveys/acs/data.html)
- 391 19. Besag J, York J, Mollié A. Bayesian image restoration, with two applications in spatial
- 392 statistics. *Ann Inst Stat Math.* Published online 1991. doi:10.1007/BF00116466
- 393 20. Simpson D, Rue H, Riebler A, Martins TG, Sørbye SH. Penalising model component
- 394 complexity: A principled, practical approach to constructing priors. *Stat Sci.* 2017;32(1):1-
- 395 28. doi:10.1214/16-STS576
- 396 21. Riebler A, Sørbye SH, Simpson D, et al. An intuitive Bayesian spatial model for disease
- 397 mapping that accounts for scaling. *Stat Methods Med Res.* 2016;25(4):1145-1165.
- 398 doi:10.1177/0962280216660421
- 399 22. Lawson AB. *Bayesian Disease Mapping: Hierarchical Modeling in Spatial Epidemiology,*
- 400 *3rd Edition.*; 2018.
- 401 23. Rue H, Martino S. Approximate Bayesian inference for latent Gaussian models by using
- 402 integrated nested Laplace approximations. *J R Stat Soc Ser B Stat Methodol.*
- 403 2009;71(2):319-392.
- 404 24. Rue H, Riebler A, Sørbye SH, Illian JB, Simpson DP, Lindgren FK. Bayesian computing with
- 405 INLA: A review. *Annu Rev Stat Its Appl.* 2017;4:395-421. doi:10.1146/annurev-statistics-
- 406 060116-054045
- 407 25. Blangiardo M, Cameletti M, Baio G, Rue H. Spatial and spatio-temporal models with R-
- 408 INLA. *Spat Spatiotemporal Epidemiol.* 2013;7:39-55. doi:10.1016/j.sste.2013.07.003

- 409 26. Larochelle MR, Slavova S, Root ED, et al. Disparities in Opioid Overdose Death Trends by
410 Race/Ethnicity, 2018-2019, from the HEALing Communities Study. *Am J Public Health*.
411 2021;111(10):1851-1854. doi:10.2105/AJPH.2021.306431
- 412 27. Lippold KM, Jones CM, Olsen EO, Giroir BP. Racial/Ethnic and Age Group Differences in
413 Opioid and Synthetic Opioid–Involved Overdose Deaths Among Adults Aged ≥18 Years in
414 Metropolitan Areas — United States, 2015–2017. *MMWR Morb Mortal Wkly Rep*.
415 2019;68(43):967-973. doi:10.15585/mmwr.mm6843a3
- 416 28. Townsend T, Kline D, Rivera-Aguirre A, et al. Racial/Ethnic and Geographic Trends in
417 Combined Stimulant/Opioid Overdoses, 2007–2019. *Am J Epidemiol*. 2022;191(4):599-
418 612. doi:10.1093/aje/kwab290
- 419 29. R.M. G, P. M, P. S. Fentanyl Law Enforcement Submissions and Increases in Synthetic
420 Opioid-Involved Overdose Deaths - 27 States, 2013-2014. *MMWR Morb Mortal Wkly*
421 *Rep*. 2016;65(33):837-843.
422 [http://www.embase.com/search/results?subaction=viewrecord&from=export&id=L6164](http://www.embase.com/search/results?subaction=viewrecord&from=export&id=L616449279%0Ahttp://dx.doi.org/10.15585/mmwr.mm6533a2)
423 [49279%0Ahttp://dx.doi.org/10.15585/mmwr.mm6533a2](http://dx.doi.org/10.15585/mmwr.mm6533a2)
- 424 30. Hu K, Klinkenberg B, Gan WQ, Slaunwhite AK. Spatial-temporal trends in the risk of illicit
425 drug toxicity death in British Columbia. *BMC Public Health*. 2022;22(1):1-11.
426 doi:10.1186/s12889-022-14586-8
427

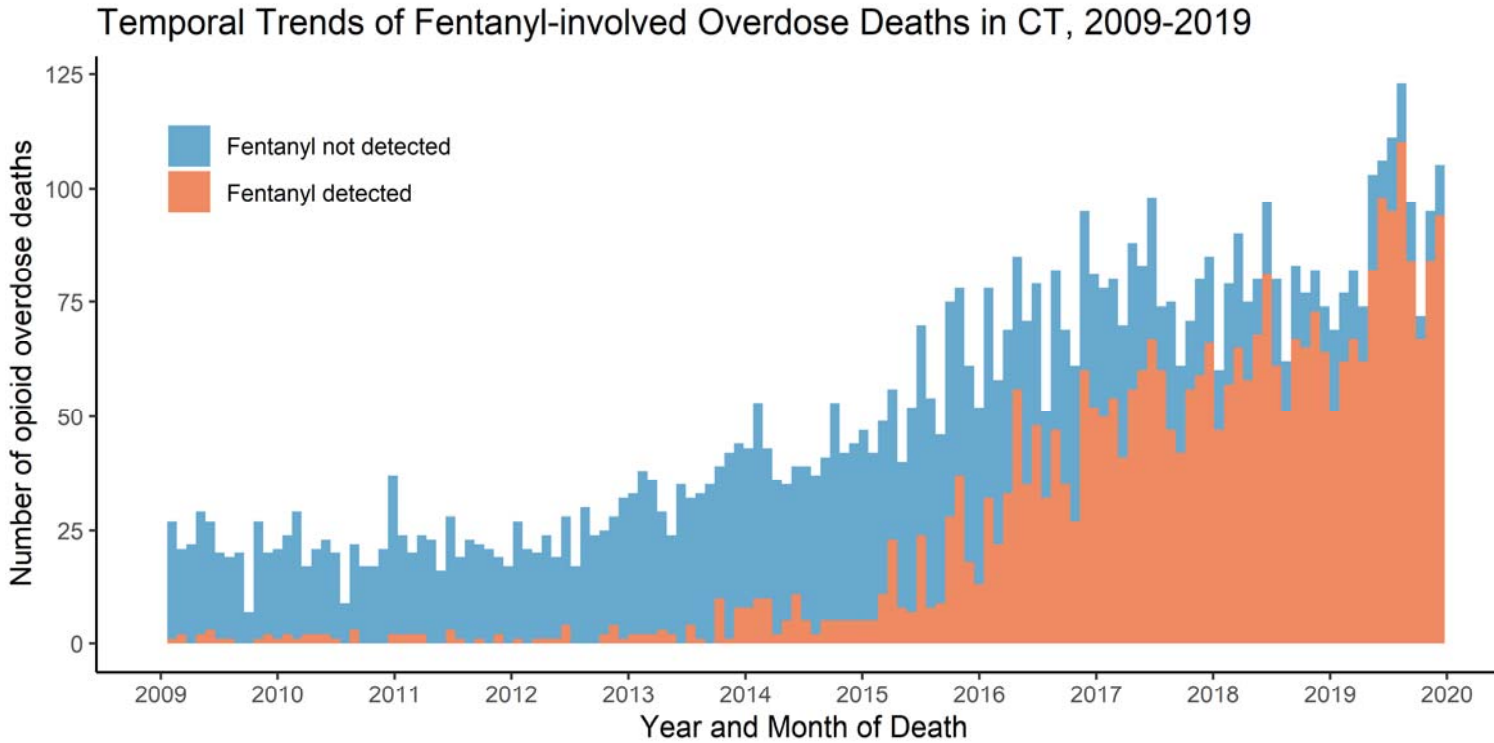
428 Table 1. Characteristics of fentanyl-detected overdose deaths among Connecticut residents, 2009-2019

	Fentanyl-detected Overdose deaths	Non-fentanyl Overdose deaths	Total sample
	n=3234	n=3398	n=6632
Age at death (years), No. (%)			
<25	260 (8.0)	287 (8.4)	547 (8.2)
25-34	879 (27.2)	775 (22.8)	1654 (24.9)
35-44	854 (26.4)	785 (23.1)	1639 (24.7)
45-54	718 (22.2)	923 (27.2)	1641 (24.7)
55-64	461 (14.3)	533 (15.7)	994 (15.0)
65+	62 (1.9)	95 (2.8)	157 (2.4)
Female, No. (%)	697 (21.6)	1025 (30.2)	1722 (26.0)
Race/ethnicity, No. (%)			
White, non-Hispanic	2445 (75.6)	2823 (83.1)	5268 (79.4)
Black, non-Hispanic	293 (9.1)	197 (5.8)	490 (7.4)
Hispanic	445 (13.8)	338 (9.9)	783 (11.8)
Other ^a	51 (1.6)	40 (1.2)	91 (1.4)
Substance present, No. (%)			
Heroin/morphine	1430 (44.3)	2000 (61.0)	3430 (51.7)
Pharmaceutical opioids ^b	320 (9.9)	990 (29.1)	1310 (19.8)
Methadone	202 (6.2)	573 (16.9)	775 (11.7)
Buprenorphine	72 (2.2)	92 (2.7)	164 (2.5)
Benzodiazepine	897 (27.7)	1276 (37.6)	2173 (32.8)
Cocaine	1265 (39.1)	773 (22.7)	2038 (30.7)
Ethanol	951 (29.4)	1032 (30.4)	1983 (29.9)
Amphetamine	141 (4.4)	105 (3.1)	246 (3.7)
Xylazine	73 (2.3)	1 (0.0)	74 (1.1)
Gabapentin	241 (7.5)	125 (3.7)	366 (5.5)
Mitragynine	31 (1.0)	10 (0.3)	41 (0.6)

429 ^a Other includes Asian, American Indian, bi-racial, or other racial/ethnic groups

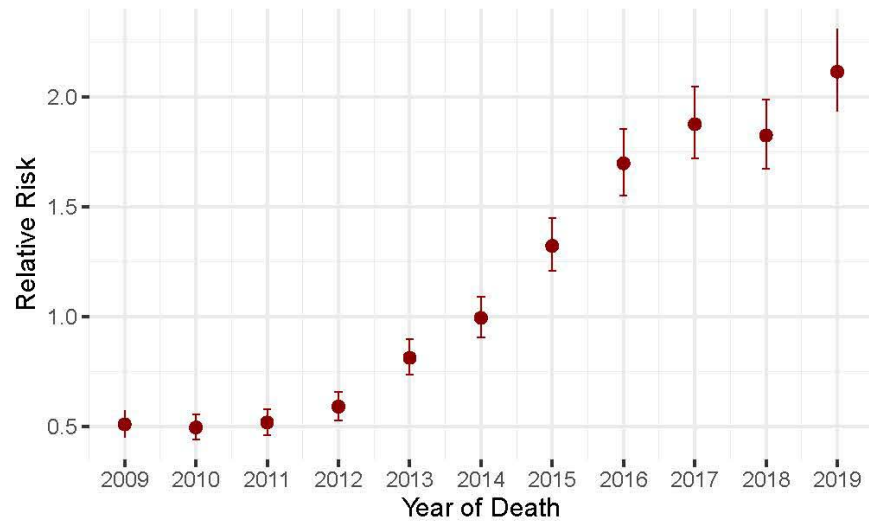
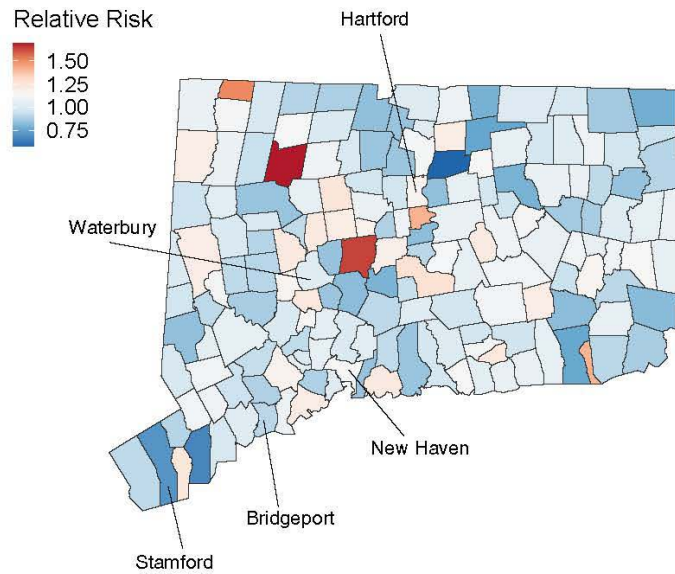
430 ^b Pharmaceutical opioids include di-H-codeine, hydromorphone, hydrocodone, oxycodone, and tramadol, but
 431 do not include methadone and buprenorphine

432 Figure 1. Monthly temporal trend fentanyl-detected overdose deaths among Connecticut residents, 2009-2019. This stacked figure
433 shows, as the number of overdose deaths increased, the share of overdose deaths involving fentanyl increased as well.
434
435



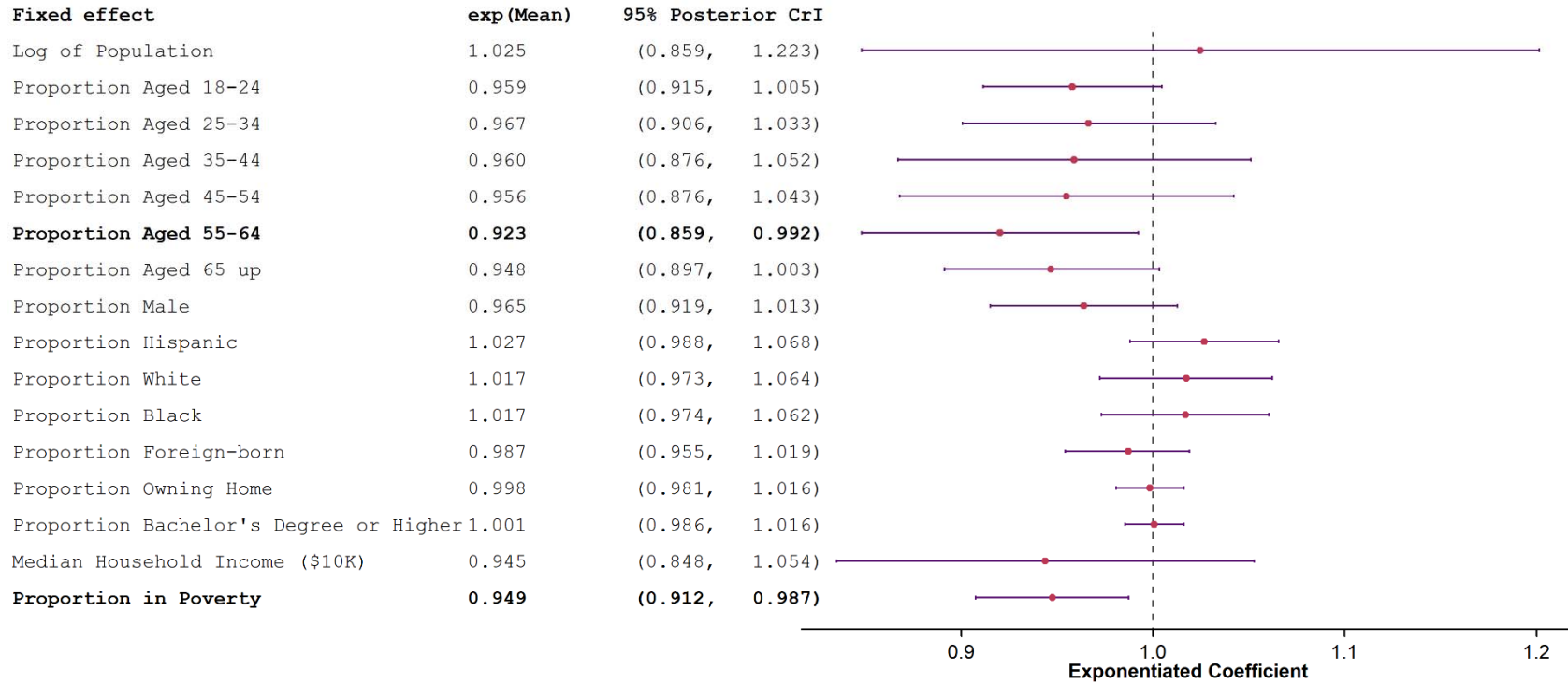
436
437

438 Figure 2: Posterior distributions of estimated parameters for spatial (α_i) and temporal (γ_t) random effects (relative risk) from the
 439 Bayesian space-time Poisson model for overall opioid-detected overdose deaths. The left panel depicts the spatial patterns of overall
 440 opioid-detected overdose deaths when holding temporal terms and other covariates constant. The right panel depicts the temporal
 441 patterns of overall opioid-detected overdose deaths when holding spatial terms and other covariates constant. The random effects
 442 were exponentiated. Larger values of relative risk indicate the higher risk of opioid-detected overdose deaths at town level in
 443 Connecticut. Note: link to the Connecticut Towns Index Map (<https://portal.ct.gov/-/media/DEEP/gis/Resources/IndexTowns.pdf>)



444

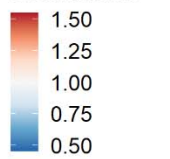
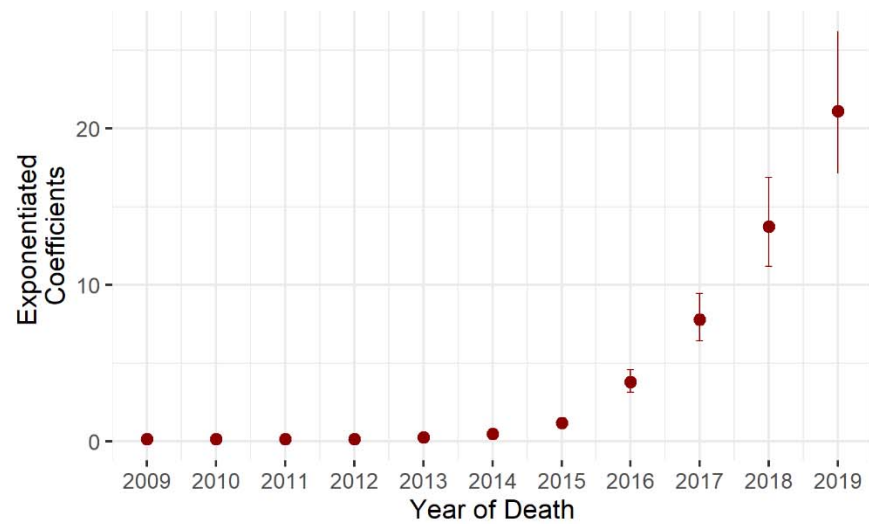
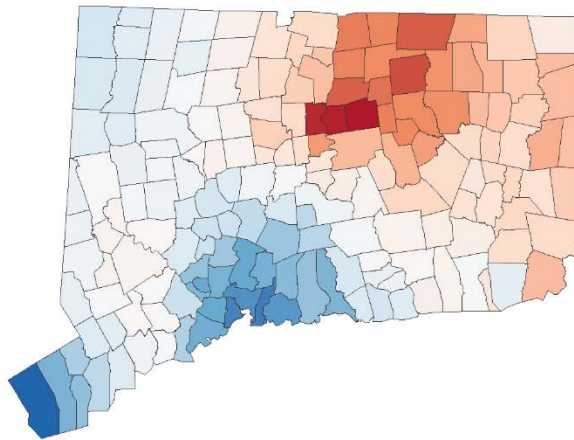
445 Figure 3. Summary of the posterior means and 95% credible intervals (CrIs) of the fixed effect coefficients of covariates. The
 446 regression coefficients are exponentiated to represent exponentiated coefficients from binomial logistic regression.



447
 448

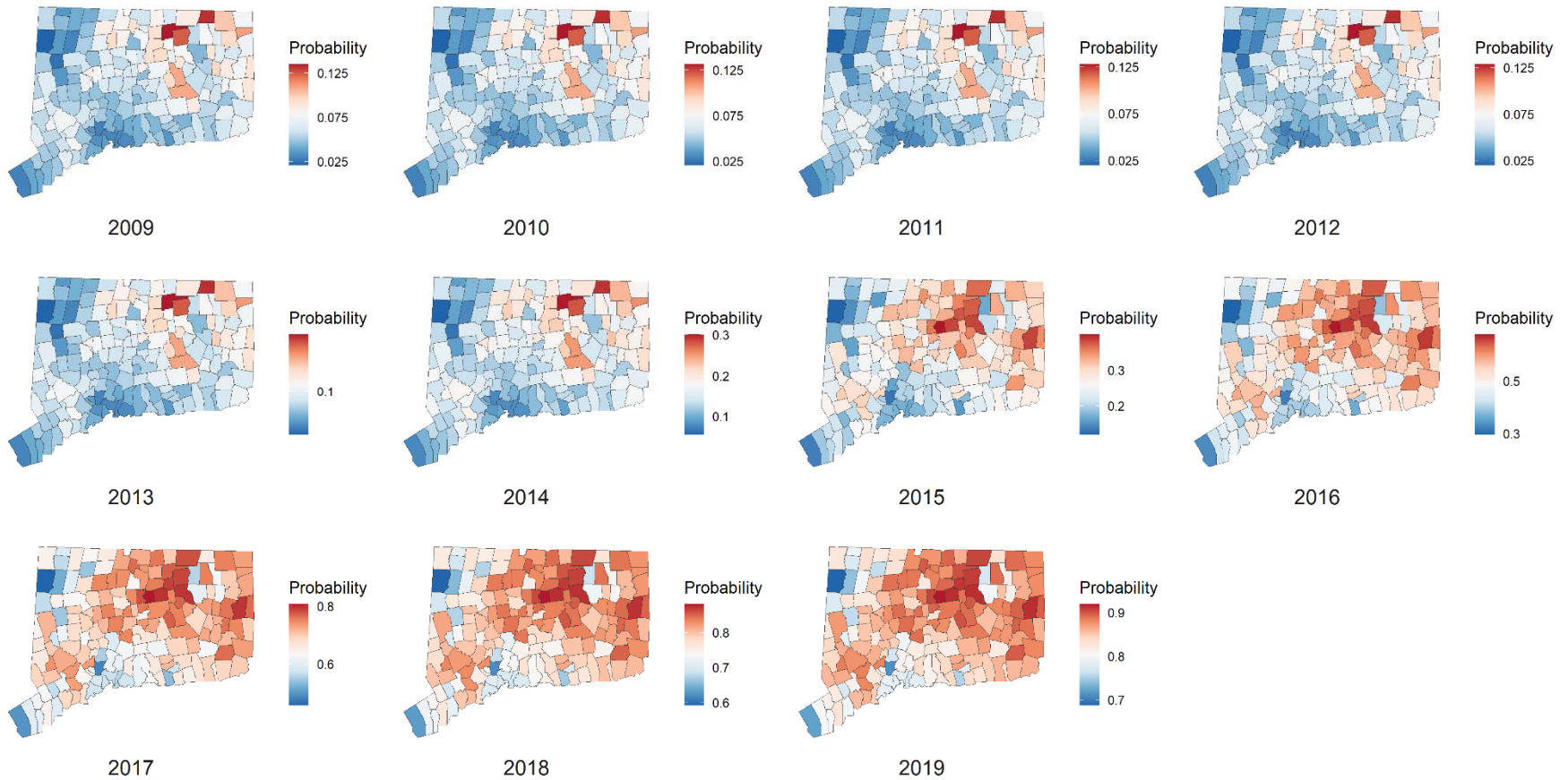
449 Figure 4: Posterior distributions of estimated parameters for spatial (μ_i) and temporal (φ_t) random effects from the Bayesian space-
 450 time binomial model for fentanyl-detected overdose deaths. The left panel depicts the spatial patterns of fentanyl-detected
 451 overdose deaths when holding temporal terms and other covariates constant. The right panel depicts the temporal patterns of
 452 fentanyl-detected overdose deaths when holding spatial terms and other covariates constant. The random effects were
 453 exponentiated. Larger values of exponentiated coefficients indicate the higher probability being fentanyl detected given an opioid
 454 overdose death at town level in Connecticut. Note: link to the Connecticut Towns Index Map ([https://portal.ct.gov/-](https://portal.ct.gov/-/media/DEEP/gis/Resources/IndexTownspdf.pdf)
 455 [/media/DEEP/gis/Resources/IndexTownspdf.pdf](https://portal.ct.gov/-/media/DEEP/gis/Resources/IndexTownspdf.pdf))

Exponentiated
Coefficients

456
457

458 Figure 5. The predicted probability of an overdose death being fentanyl-detected from the Bayesian space-time binomial model,
459 stratified by town and calendar year, Connecticut. Color scales differ by year to show the distribution within each year. Note: link to
460 the Connecticut Towns Index Map (<https://portal.ct.gov/-/media/DEEP/gis/Resources/IndexTownspdf.pdf>)



461
462

463 **Appendix**

464 **Appendix S1**

465 **Priors on random effects in Bayesian space-time Poisson model for overall opioid-detected overdose deaths**

$$\log(\lambda_{it}) = \mathbf{x}_{it}^T \boldsymbol{\beta} + \alpha_i + \gamma_t + \delta_{it} + \log(\text{pop}_n)$$

$$\alpha_i = u_i + v_i, \quad u_i \sim N(0, \tau_u^{-1} Q^-), \quad v_i \sim N(0, \tau_v^{-1} I)$$

$$\gamma_t = \Delta\pi_i + \rho_t, \quad \Delta\pi_i = \pi_i - \pi_{i-1} \sim N(0, \tau_\pi^{-1}), \quad \rho_t \sim N(0, \tau_\rho^{-1} I),$$

466 where $u_i \sim N(0, \tau_u^{-1} Q)$ represents the spatial structured random effect and is modeled under the class of intrinsic Gaussian Markov
467 random fields models. Q denotes the precision matrix (neighboring matrix), and Q^- is the generalized inverse of the matrix Q . The
468 marginal variances are $\tau_u^{-1} [Q^-]_{ii}$, which are dependent on the matrix Q . $v_i \sim N(0, \tau_v^{-1} I)$ is the spatial unstructured random effect
469 and τ_v^{-1} is the marginal variance. Gamma priors with small rate parameters are commonly assigned to τ_u and τ_v . Here, Gamma(1,
470 0.0005) is considered.

471

472 $\Delta\pi_i = \pi_i - \pi_{i-1} \sim N(0, \tau_\pi^{-1})$ is first order random walk temporal random effect defined as a random step at each point in time ($\Delta\pi_i$).
473 All random steps are independent and identically distributed. $\rho_t \sim N(0, \tau_\rho^{-1} I)$ is the temporal unstructured random effect and τ_ρ^{-1} is
474 the marginal variance. Gamma priors with small rate parameters are commonly assigned to τ_π and τ_ρ . Here, Gamma(1, 0.0005) is
475 considered.

476

477 **Appendix S2: Model Comparison**

478 **Appendix S2.1: Model Comparison for overall opioid-detected overdose deaths**

479 For overall opioid-detected overdose deaths, Poisson models were used to estimate the mean number of opioid-detected overdose
 480 deaths in each town at each year from 2009-2019. Concerning some towns with 0 opioid-detected overdose deaths, zero-inflated
 481 Poisson models were also examined. Deviance information criterion (DIC) and Watanabe-Akaike information criterion were used to
 482 compare Poisson model and zero-inflated Poisson model.
 483

484 Appendix S2. Table 1: Model Comparison for overall opioid-detected overdose deaths

Model	DIC	WAIC
Poisson (in the main text)	5726.50	5733.06
Zero-inflated Poisson	6525.00	6528.64

485
 486 Based on DIC and WAIC, Poisson model is selected.
 487

488 **Appendix S2.2: Model Comparison for fentanyl-detected overdose deaths**

489 For fentanyl-detected overdose death among all opioid-detected overdose deaths, binomial model and logistic regression were used
 490 to estimate the probability being fentanyl-detected given an opioid overdose death in each town at each year from 2009-2019.
 491 Several parsimonious models, in addition to the logistic model mentioned in the main text were examined. DIC and WAIC were used
 492 for model comparison.
 493

494 Appendix S2. Table 2: Model Comparison for fentanyl-detected overdose deaths

Model	DIC	WAIC
Conditional autoregressive term at town level + linear calendar year + unstructured temporal term for calendar year + demographic covariates	2175.64	2182.10
Conditional autoregressive term at town level + first-order random walk structured temporal term for calendar year + demographic covariates	2172.43	2178.53
Conditional autoregressive term at town	2172.51	2178.61

level + first-order random walk structured temporal term for calendar year + unstructured temporal term for calendar year + demographic covariates		
Conditional autoregressive term at town level + first-order random walk structured temporal term for calendar year + space-time interaction term + demographic covariates	2172.39	2178.49
Conditional autoregressive term at town level + first-order random walk structured temporal term for calendar year + unstructured temporal term for calendar year + space-time interaction term + demographic covariates (model specified in the main text)	2172.44	2178.53

495
 496 Based on DIC and WAIC, the binomial model including conditional autoregressive term at town level, first-order random walk
 497 structured temporal term for calendar year, space-time interaction term, and demographic covariates, without unstructured
 498 temporal term, was selected.
 499

500 **Appendix S3**

501 **Sensitivity analysis using penalized complexity (PC) priors for Bayesian space-time Poisson model for overall opioid-detected**
502 **overdose deaths**

503 In this sensitivity analysis, instead of using gamma priors for precision hyperparameters in Bayesian space-time Poisson model for
504 overall opioid-detected overdose deaths, we employed penalized complexity (PC)¹ priors for the prior distribution of
505 hyperparameters. The hyperprior distributions are chosen with the PC framework.² We let the precision parameters τ_w , τ_v , τ_π and τ_ρ
506 (as described in Appendix S1) $\sim PC(0.2/0.31, 0.01)$, which corresponds to $Pr(1/\sqrt{\tau} > 0.2/0.31) = 0.01$, leading to the prior
507 standard deviation of the marginal log relative risk being 0.2. The results of this sensitivity analysis were shown in Appendix S3
508 Figure 1.

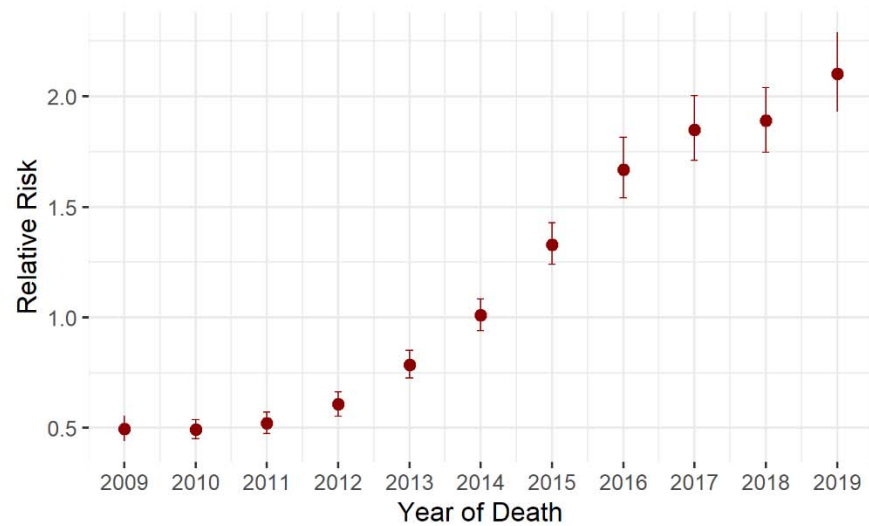
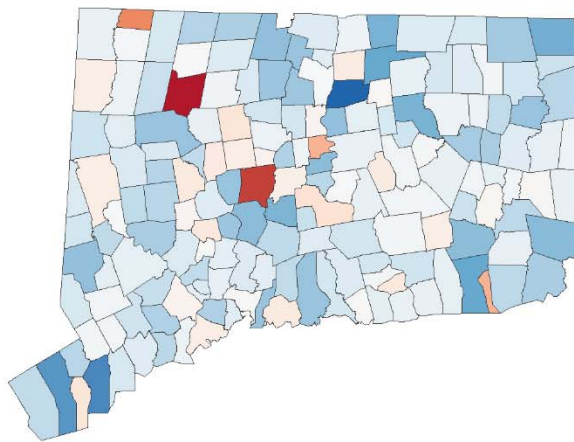
509

510 References:

- 511 1. Simpson D, Rue H, Riebler A, Martins TG, Sørbye SH. Penalising model component complexity: A principled, practical approach to
512 constructing priors. Stat Sci. 2017;32(1):1-28.
- 513 2. Riebler A, Sørbye SH, Simpson D, et al. An intuitive Bayesian spatial model for disease mapping that accounts for scaling. Stat
514 Methods Med Res. 2016;25(4):1145-1165.

515 Appendix S3. Figure 1: Posterior distributions of estimated parameters for spatial (α_i) and temporal (γ_t) random effects (relative
 516 risk) from the Bayesian space-time Poisson model for overall opioid-detected overdose deaths using penalized complexity priors for
 517 hyperparameters. The left panel depicts the spatial patterns of overall opioid-detected overdose deaths when holding temporal
 518 terms and other covariates constant. The right panel depicts the temporal patterns of overall opioid-detected overdose deaths when
 519 holding spatial terms and other covariates constant. The random effects were exponentiated. Larger values of relative risk indicate
 520 the higher risk of opioid-detected overdose deaths at town level in Connecticut. Note: link to the Connecticut Towns Index Map
 521 (<https://portal.ct.gov/-/media/DEEP/gis/Resources/IndexTownspdf.pdf>)

Relative Risk



522
523
524

525 **Appendix S4**526 **Appendix S4. Table 1. Characteristics of opioid-detected overdose deaths among Connecticut residents by year, 2009-2019**

Year	2009	2010	2011	2012	2013	2014	2015	2016	2017	2018	2019
	n=266	n=254	n=268	n=298	n=429	n=510	n=678	n=883	n=960	n=949	n=1138
Age at death (years), No. (%)											
<25	28 (10.5)	26 (10.2)	39 (14.6)	39 (13.1)	48 (11.2)	31 (6.1)	60 (8.8)	65 (7.4)	79 (8.2)	68 (7.2)	64 (5.6)
25-34	62 (23.3)	45 (17.7)	75 (28.1)	74 (24.8)	106 (24.7)	131 (25.7)	167 (24.6)	233 (26.4)	264 (27.5)	226 (23.8)	271 (23.8)
35-44	81 (30.5)	72 (28.3)	58 (21.7)	60 (20.1)	95 (22.1)	132 (25.9)	146 (21.5)	200 (22.7)	239 (24.9)	248 (26.1)	308 (27.1)
45-54	64 (24.1)	91 (35.8)	64 (24.0)	87 (29.2)	113 (26.3)	142 (27.8)	173 (25.5)	225 (25.5)	213 (22.2)	229 (24.1)	240 (21.1)
55-64	29 (10.9)	20 (7.9)	30 (11.2)	30 (10.1)	62 (14.5)	59 (11.6)	110 (16.2)	144 (16.3)	148 (15.4)	148 (15.6)	214 (18.8)
≥65	2 (0.8)	0 (0.0)	1 (0.4)	8 (2.7)	5 (1.2)	15 (2.9)	22 (3.2)	16 (1.8)	17 (1.8)	30 (3.2)	41 (3.6)
Female, No. (%)	83 (31.2)	79 (31.1)	76 (28.5)	80 (26.8)	127 (29.6)	154 (30.2)	178 (26.3)	228 (25.8)	232 (24.2)	222 (23.4)	263 (23.1)
Race/ethnicity, No. (%)											
White, non-Hispanic	228 (85.7)	214 (84.3)	236 (88.4)	245 (82.2)	357 (83.2)	430 (84.3)	562 (82.9)	696 (78.8)	764 (79.6)	710 (74.8)	826 (72.6)
Black, non-Hispanic	12 (4.5)	13 (5.1)	9 (3.4)	20 (6.7)	26 (6.1)	21 (4.1)	36 (5.3)	64 (7.2)	72 (7.5)	94 (9.9)	123 (10.8)
Hispanic	25 (9.4)	26 (10.2)	20 (7.5)	28 (9.4)	42 (9.8)	56 (11.0)	74 (10.9)	102 (11.6)	111 (11.6)	127 (13.4)	172 (15.1)
Other ^a	1 (0.4)	1 (0.4)	2 (0.7)	5 (1.7)	4 (0.9)	3 (0.6)	6 (0.9)	21 (2.4)	13 (1.4)	18 (1.9)	17 (1.5)
Substance present, No. (%)											
Fentanyl/fentanyl analogs	15 (5.6)	14 (5.5)	14 (5.2)	15 (5.0)	36 (8.4)	75 (14.7)	183 (27.0)	472 (53.5)	670 (69.8)	763 (80.4)	977 (85.9)
Heroin/morphine	146 (54.9)	124 (48.8)	144 (53.9)	181 (60.7)	278 (64.8)	335 (65.7)	432 (63.7)	522 (59.1)	463 (48.2)	399 (42.0)	406 (35.7)
Pharmaceutical opioids ^b	96 (36.1)	96 (37.8)	80 (30.0)	81 (27.2)	108 (25.2)	142 (27.8)	162 (23.9)	155 (17.6)	149 (15.5)	107 (11.3)	134 (11.8)
Methadone	66 (24.8)	58 (22.8)	55 (20.6)	37 (12.4)	48 (11.2)	54 (10.6)	81 (11.9)	96 (10.9)	100 (10.4)	84 (8.9)	96 (8.4)
Buprenorphine	0 (0.0)	0 (0.0)	0 (0.0)	0 (0.0)	7 (1.6)	9 (1.8)	21 (3.1)	30 (3.4)	25 (2.6)	29 (3.1)	43 (3.8)
Benzodiazepine	62 (23.3)	84 (33.1)	93 (34.8)	48 (16.1)	131 (30.5)	225 (44.1)	285 (42.0)	304 (34.4)	345 (35.9)	284 (29.9)	312 (27.4)
Cocaine	38 (14.3)	34 (13.4)	64 (24.0)	67 (22.5)	113 (26.3)	118 (23.1)	162 (23.9)	263 (29.8)	333 (34.7)	365 (38.5)	481 (42.3)
Ethanol	69 (25.9)	76 (29.9)	87 (32.6)	60 (20.1)	114 (26.6)	155 (30.4)	188 (27.7)	274 (31.0)	321 (33.4)	274 (28.9)	365 (32.1)
Amphetamine	1 (0.4)	1 (0.4)	3 (1.1)	5 (1.7)	5 (1.2)	22 (4.3)	35 (5.2)	29 (3.3)	35 (3.6)	48 (5.1)	62 (5.4)
Xylazine	0 (0.0)	0 (0.0)	0 (0.0)	0 (0.0)	0 (0.0)	0 (0.0)	0 (0.0)	0 (0.0)	0 (0.0)	0 (0.0)	74 (6.5)
Gabapentin	0 (0.0)	0 (0.0)	1 (0.4)	0 (0.0)	0 (0.0)	0 (0.0)	2 (0.3)	50 (5.7)	85 (8.9)	77 (8.1)	151 (13.3)
Mitragynine	0 (0.0)	0 (0.0)	0 (0.0)	0 (0.0)	0 (0.0)	1 (0.2)	0 (0.0)	8 (0.9)	3 (0.3)	7 (0.7)	22 (1.9)

^a Other includes Asian, American Indian, bi-racial, or other racial/ethnic groups

^b Pharmaceutical opioids include di-H-codeine, hydromorphone, hydrocodone, oxycodone, and tramadol, but do not include methadone and buprenorphine

527
528
529

530 **Appendix S4. Table 2. Characteristics of fentanyl-detected overdose deaths among Connecticut residents by year, 2009-2019**

Year	2009	2010	2011	2012	2013	2014	2015	2016	2017	2018	2019
	n=266	n=254	n=268	n=298	n=429	n=510	n=678	n=883	n=960	n=949	n=1138
Age at death (years), No. (%)											
<25	2 (13.3)	1 (7.1)	4 (28.6)	1 (6.7)	2 (5.6)	7 (9.3)	19 (10.4)	35 (7.4)	64 (9.6)	63 (8.3)	62 (6.3)
25-34	3 (20.0)	4 (28.6)	4 (28.6)	3 (20.0)	6 (16.7)	21 (28.0)	50 (27.3)	136 (28.8)	209 (31.2)	195 (25.6)	248 (25.4)
35-44	2 (13.3)	2 (14.3)	3 (21.4)	1 (6.7)	8 (22.2)	25 (33.3)	43 (23.5)	122 (25.8)	175 (26.1)	201 (26.3)	272 (27.8)
45-54	4 (26.7)	6 (42.9)	1 (7.1)	6 (40.0)	12 (33.3)	16 (21.3)	47 (25.7)	111 (23.5)	138 (20.6)	177 (23.2)	200 (20.5)
55-64	4 (26.7)	1 (7.1)	2 (14.3)	3 (20.0)	8 (22.2)	4 (5.3)	22 (12.0)	61 (12.9)	79 (11.8)	110 (14.4)	167 (17.1)
≥65	0 (0.0)	0 (0.0)	0 (0.0)	1 (6.7)	0 (0.0)	2 (2.7)	2 (1.1)	7 (1.5)	5 (0.7)	17 (2.2)	28 (2.9)
Female, No. (%)	9 (60.0)	4 (28.6)	4 (28.6)	5 (33.3)	12 (33.3)	25 (33.3)	34 (18.6)	94 (19.9)	136 (20.3)	162 (21.2)	212 (21.7)
Race/ethnicity, No. (%)											
White, non-Hispanic	12 (80.0)	11 (78.6)	13 (92.9)	14 (93.3)	26 (72.2)	61 (81.3)	149 (81.4)	370 (78.4)	523 (78.1)	568 (74.4)	698 (71.4)
Black, non-Hispanic	1 (6.7)	1 (7.1)	0 (0.0)	0 (0.0)	4 (11.1)	4 (5.3)	9 (4.9)	33 (7.0)	55 (8.2)	79 (10.4)	107 (11.0)
Hispanic	2 (13.3)	2 (14.3)	1 (7.1)	1 (6.7)	6 (16.7)	9 (12.0)	23 (12.6)	62 (13.1)	82 (12.2)	101 (13.2)	156 (16.0)
Other ^a	0 (0.0)	0 (0.0)	0 (0.0)	0 (0.0)	0 (0.0)	1 (1.3)	2 (1.1)	7 (1.5)	10 (1.5)	15 (2.0)	16 (1.6)
Substance present, No. (%)											
Heroin/morphine	2 (13.3)	1 (7.1)	2 (14.3)	1 (6.7)	11 (30.6)	38 (50.7)	112 (61.2)	277 (58.7)	321 (47.9)	313 (41.0)	352 (36.0)
Pharmaceutical opioids ^b	4 (26.7)	2 (14.3)	4 (28.6)	3 (20.0)	6 (16.7)	14 (18.7)	25 (13.7)	53 (11.2)	66 (9.9)	60 (7.9)	83 (8.5)
Methadone	2 (13.3)	2 (14.3)	0 (0.0)	1 (6.7)	3 (8.3)	5 (6.7)	6 (3.3)	33 (7.0)	43 (6.4)	40 (5.2)	67 (6.9)
Buprenorphine	0 (0.0)	0 (0.0)	0 (0.0)	0 (0.0)	0 (0.0)	1 (1.3)	6 (3.3)	12 (2.5)	10 (1.5)	16 (2.1)	27 (2.8)
Benzodiazepine	4 (26.7)	3 (21.4)	4 (28.6)	2 (13.3)	9 (25.0)	23 (30.7)	56 (30.6)	127 (26.9)	208 (31.0)	213 (27.9)	248 (25.4)
Cocaine	3 (20.0)	2 (14.3)	3 (21.4)	1 (6.7)	16 (44.4)	19 (25.3)	50 (27.3)	157 (33.3)	254 (37.9)	320 (41.9)	440 (45.0)
Ethanol	1 (6.7)	4 (28.6)	3 (21.4)	0 (0.0)	9 (25.0)	14 (18.7)	47 (25.7)	140 (29.7)	214 (31.9)	215 (28.2)	304 (31.1)
Amphetamine	0 (0.0)	0 (0.0)	0 (0.0)	0 (0.0)	0 (0.0)	2 (2.7)	10 (5.5)	13 (2.8)	19 (2.8)	41 (5.4)	56 (5.7)
Xylazine	0 (0.0)	0 (0.0)	0 (0.0)	0 (0.0)	0 (0.0)	0 (0.0)	0 (0.0)	0 (0.0)	0 (0.0)	0 (0.0)	73 (7.5)
Gabapentin	0 (0.0)	0 (0.0)	0 (0.0)	0 (0.0)	0 (0.0)	0 (0.0)	0 (0.0)	22 (4.7)	48 (7.2)	50 (6.6)	121 (12.4)
Mitragynine	0 (0.0)	0 (0.0)	0 (0.0)	0 (0.0)	0 (0.0)	0 (0.0)	0 (0.0)	3 (0.6)	2 (0.3)	5 (0.7)	21 (2.1)

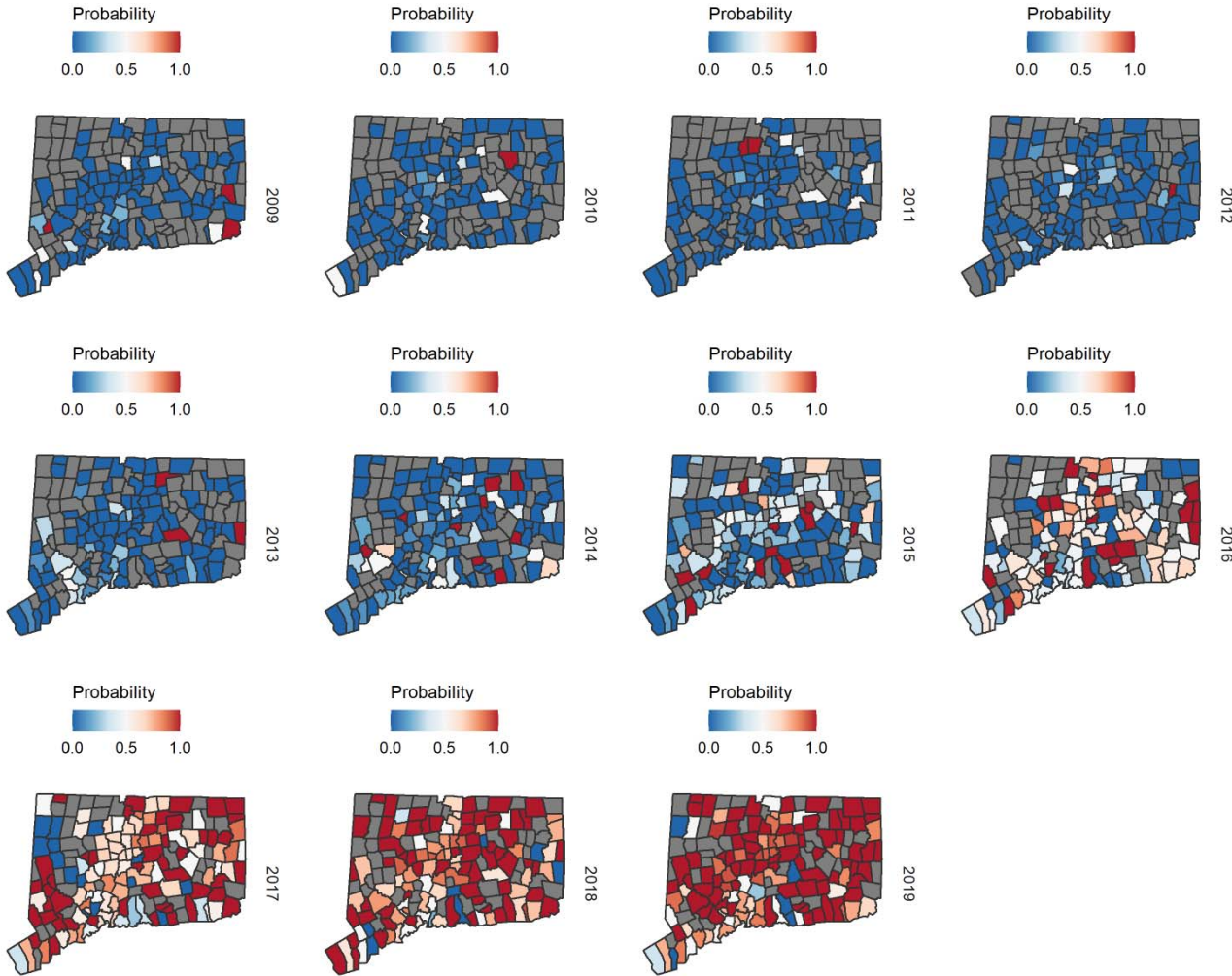
^a Other includes Asian, American Indian, bi-racial, or other racial/ethnic groups

^b Pharmaceutical opioids include di-H-codeine, hydromorphone, hydrocodone, oxycodone, and tramadol, but do not include methadone and buprenorphine

531
532
533

534 **Appendix S5**

535 Appendix S5. Figure 1. Spatial patterns of observed proportion being fentanyl-detected among opioid overdose deaths at the
536 city/town level, stratified by year, 2009-2019. Towns with grey color represent no opioid-detected deaths. Note: link to the
537 Connecticut Towns Index Map (<https://portal.ct.gov/-/media/DEEP/gis/Resources/IndexTownspdf.pdf>)



538
539

540 **Appendix S6**

541 **Sensitivity Analysis 1**

542 Poisson model was used as an alternative to binomial model to estimate the risk of fentanyl-detected overdose deaths among
543 opioid-detected overdose deaths at town level in Connecticut, 2009-2019. Specifically, we modelled the number of fentanyl-
544 detected overdose deaths y_{it} in town i during year t as independently and identically Poisson distributed variables with mean μ_{it} ,

$$y_{it} \sim \text{Poisson}(\mu_{it})$$

545 Then the logarithm of the mean number of fentanyl-detected overdose deaths (μ_{it}) is modeled as

$$\log(\mu_{it}) = \mathbf{x}_{it}^T \boldsymbol{\beta} + \alpha_i + \varphi_t + \delta_{it} + \log(od_n)$$

546 where \mathbf{x}_{it} is the vector of covariates for town i at year t (including the time-varying and space-varying variables from ACS as
547 aforementioned), and $\boldsymbol{\beta}$ is a vector of fixed effect coefficients for \mathbf{x}_{it} . In addition, α_i in the model is town-level spatial main effect,
548 φ_t is the yearly temporal main effect, and δ_{it} is the interaction term between space (town level) and time (year). The number of
549 overall opioid-detected overdose deaths in each town in each year was used as an offset $\log(od_n)$.

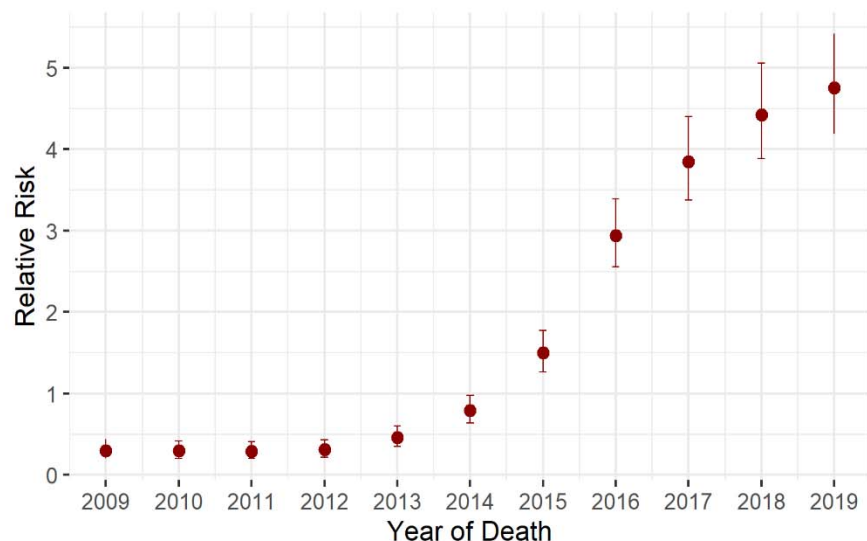
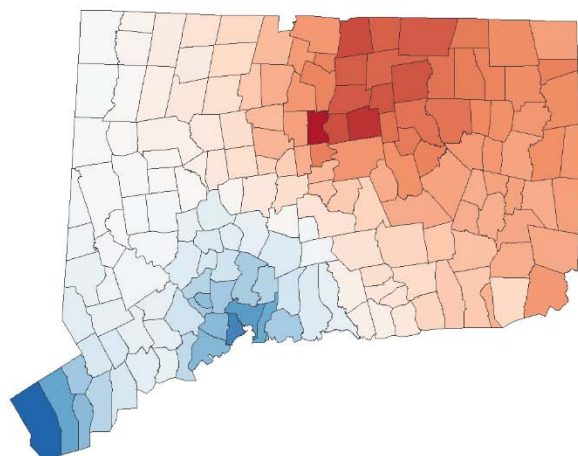
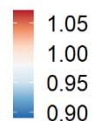
550

551 Specifically, the spatial term α_i is a random effect that follows the conditional autoregressive model proposed by Besag, York and
552 Mollie.¹⁹ The random effect can be further decomposed into two components, an intrinsic conditional autoregressive term that
553 smooths each town-level estimate by forming a weighted average with all adjacent census tracts, plus spatially unstructured
554 component that models independent location-specific error and is assumed to be independently identically normally distributed
555 across towns. The temporal trend φ_t , is modeled by the sum of two components, a first-order random walk-correlated time
556 component, and a temporally unstructured component that models independent year-specific error and is independently identically
557 and normally distributed across calendar years. The space-time interaction term δ_{it} , is modelled as an independent noise term for
558 each town and time period, and allows for temporal trends in a given towns to deviate from the overall spatial and temporal trends
559 given by α_i and φ_t , such that local patterns can emerge across time and space. The results were shown in Appendix S6 Figure 1.

560

561 Appendix S6. Figure 1. Posterior distributions of estimated parameters for spatial (α_i) and temporal (φ_t) random effects from the
562 Bayesian space-time Poisson model for fentanyl-detected overdose deaths. The random effects were exponentiated. Larger values
563 of exponentiated coefficients indicate the higher risk of being fentanyl-detected among all opioid overdose death at town level in
564 Connecticut. Note: link to the Connecticut Towns Index Map (<https://portal.ct.gov/-/media/DEEP/gis/Resources/IndexTowns.pdf>)

Relative Risk



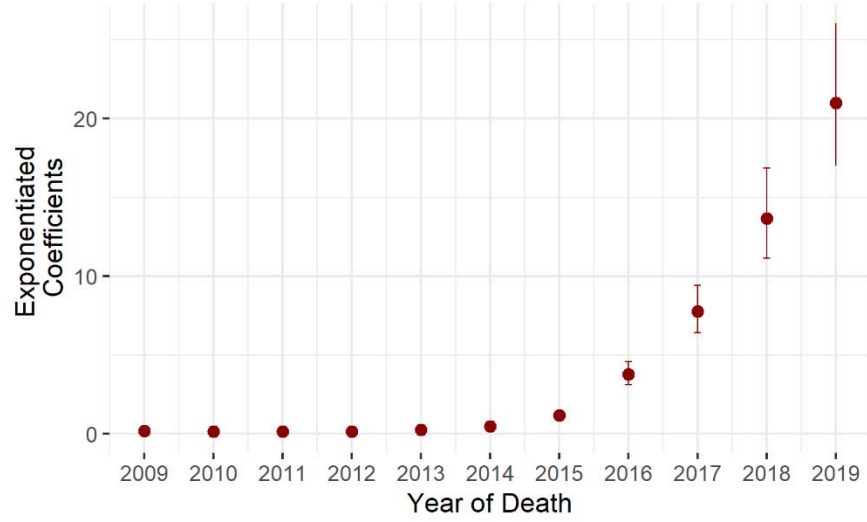
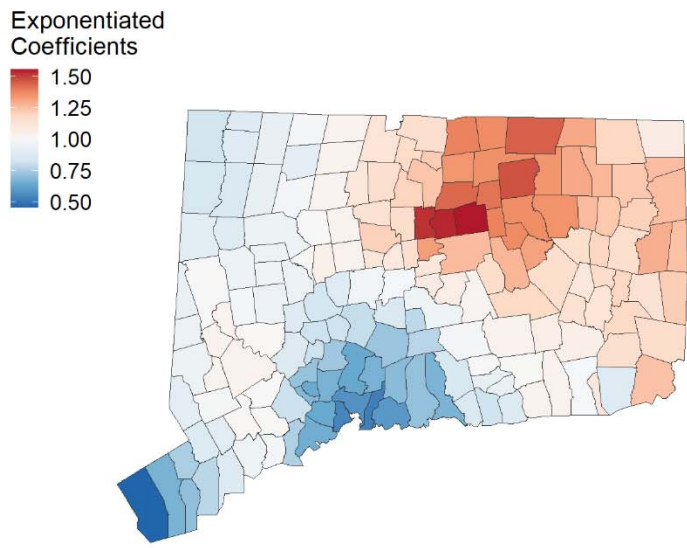
565

566

567 **Sensitivity Analysis 2**

568 In this sensitivity analysis, we still used the binomial model as described in the main text Methods section. We restricted the
569 analytical sample to adult (aged ≥ 18) opioid-detected overdose deaths, and modeled the probability of being fentanyl-detected
570 given an adult opioid overdose death in the binomial model. We included the town-level adult population size instead of the town-
571 level total population size as a covariate. As a result, 6618 adult opioid-detected overdose deaths were included in this sensitivity
572 analysis, with 18 (aged < 18) deaths excluded (4 were fentanyl-detected). The results were shown in Appendix S6 Figure 2.
573

574 Appendix S6. Figure 2. Posterior geometric means of the autoregressive spatial (μ_i) and temporal (φ_t) random effects from the
575 Bayesian space-time binomial model for adult fentanyl-detected overdose deaths. The left panel depicts the spatial patterns of adult
576 fentanyl-detected overdose deaths when holding temporal terms and other covariates constant. The right panel depicts the
577 temporal patterns of adult fentanyl-detected overdose deaths when holding spatial terms and other covariates constant. The
578 random effects were exponentiated. Larger values of exponentiated coefficients indicate the higher probability being fentanyl
579 detected given an opioid overdose death at town level in Connecticut. Note: link to the Connecticut Towns Index Map
580 (<https://portal.ct.gov/-/media/DEEP/gis/Resources/IndexTownspdf.pdf>)
581



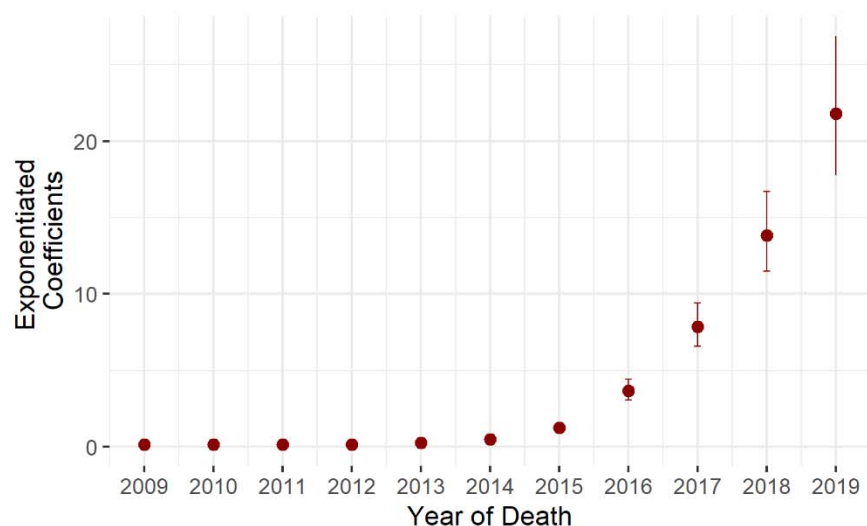
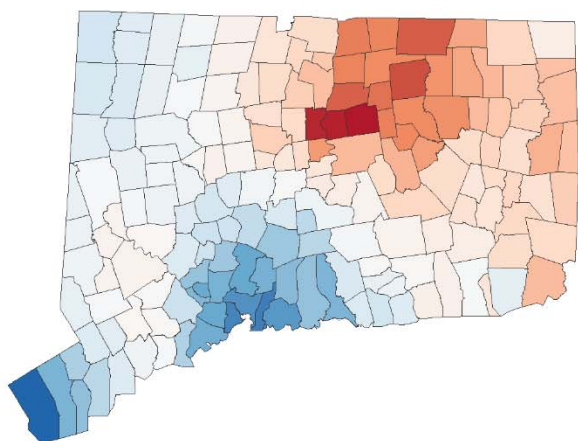
582
583

584 **Sensitivity Analysis 3**

585 In this sensitivity analysis, instead of using gamma priors for precision hyperparameters in Bayesian space-time Poisson model for
586 overall opioid-detected overdose deaths, we employed penalized complexity (PC) priors for the prior distribution of
587 hyperparameters. The hyperprior distributions are chosen with the PC framework. We let the precision parameters τ_u, τ_v, τ_π and τ_ρ
588 (as described in Appendix S1) $\sim PC(0.2/0.31, 0.01)$, which corresponds to $Pr(1/\sqrt{\tau} > 0.2/0.31) = 0.01$, leading to the prior
589 standard deviation being 0.2. The results of this sensitivity analysis were shown in Appendix S6 Figure 3.
590

591 Appendix S6. Figure 3. Posterior distributions of estimated parameters for spatial (μ_i) and temporal (φ_t) random effects from the
592 Bayesian space-time binomial model for fentanyl-detected overdose deaths using penalized complexity priors for hyperparameters.
593 The left panel depicts the spatial patterns of fentanyl-detected overdose deaths when holding temporal terms and other covariates
594 constant. The right panel depicts the temporal patterns of fentanyl-detected overdose deaths when holding spatial terms and other
595 covariates constant. The random effects were exponentiated. Larger values of exponentiated coefficients indicate the higher
596 probability being fentanyl detected given an opioid overdose death at town level in Connecticut. Note: link to the Connecticut Towns
597 Index Map (<https://portal.ct.gov/-/media/DEEP/gis/Resources/IndexTownspdf.pdf>)

Exponentiated
Coefficients



598
599